Journal of Thermal Engineering
https://jten.yildiz.edu.tr/
https://doi.org/10.47481/jten.0076

RESEARCH ARTICLE

Study the impacts of drilling on heat sink efficiency using Solidworks simulation and the response surface method

Serwan S. Mohammed Talabani[1], Ahmed T. Azeez[2], Dara Khalid Khidhir[3,*], Zanyar Q. Salih[4], Sana Wali[5], Huda Zuber[6], Chenar Ali[7], Mohsen Naje[8]

[1]Department of Mechanical and Manufacturing Engineering, Faculty of Engineering, Koya University, Koya 44023, Iraq
[2]Department of Mechanical and Manufacturing Engineering, Faculty of Engineering, Koya University, Koya 44023, Iraq
[3]Department of Mechanical and Manufacturing Engineering, Faculty of Engineering, Koya University, Koya 44023, Iraq
[4]Department of Mechanical and Manufacturing Engineering, Faculty of Engineering, Koya University, Koya 44023, Iraq
[5]Department of Manufacturing and Industrial Engineering, Faculty of Engineering, Koya University, Koya 44023, Iraq
[6]Department of Manufacturing and Industrial Engineering, Faculty of Engineering, Koya University, Koya 44023, Iraq
[7]Department of Manufacturing and Industrial Engineering, Faculty of Engineering, Koya University, Koya 44023, Iraq
[8]Department of Manufacturing and Industrial Engineering, Faculty of Engineering, Koya University, Koya 44023, Iraq

Abstract

Heat sinks are vital components for preventing overheating in electronic devices, and perfecting their performance is a key challenge due to their compact design and the need for effective heat dissipation. This paper aims to use experimentally validated simulations in SolidWorks (2023) to improve their cooling efficiency by evaluating shape factors of three designs: square, circular, and elliptical. The response surface method was used to assess the combined effects of drilling parameters (diameter, depth, and number of holes) on performance optimization. The results showed that the square shape was superior because its temperature was 44°C and 34°C lower than those of the circular and elliptical shapes, respectively. The highest Nusselt number and the lowest thermal resistance further confirmed the superiority of the square design. Additionally, drilling 195 holes of 1.5 mm diameter through the entire thickness (30 mm) of the heat sink further reduced the temperature by 19 °C compared to an undrilled square heat sink. Drilling with these dimensions increased the exposed surface area and decreased the thermally stored mass by 13.15 %, which provides a physical explanation for the observed improvements. While existing literature discusses the roles of drilling and shape factors, no studies have examined their combined influence specifically in the core of heat sinks. This study aims to integrate numerical analyses and experimental findings using statistical methods, thereby extending current research and highlighting the novelty of this work. The findings inspire engineers to develop eco-efficient passive cooling systems for electronic devices.

Keywords: CPU, heat sinks, heat transfer, SOLIDWORKS, response surface method

Cite this article as: Talabani, S. S. M., Azeez, A. T., Khidhir, D. K., Salih, Z. Q., Wali, S., Zuber, H., Ali, C., & Naje, M. (2026). Study the impacts of drilling on heat sink efficiency using Solidworks simulation and the response surface method. Journal of Thermal Engineering, 12(6), 1943–1954. https://doi.org/10.47481/jten.0076

1. Introduction

Heat sinks are essential components of electronic devices that keep temperatures within allowable ranges and prevent thermal damage [1,2]. Data centers worldwide consume approximately 2% of global energy; roughly 30%–50% of that energy is used for cooling. A primary challenge lies in producing eco-efficient units for managing the resulting thermal energy in electronics apparatus, especially microchips [3,4]. Various advanced cooling technologies, such as cold water, semiconductor, and liquid nitrogen, have been developed; however, the high cost keeps heat sinks as the most reliable and economical method [5,6].

Literature commonly regards geometrical configuration and perforation as reliable methods for developing heat sinks. Regardless of the technique, the primary goals are to increase the surface area for heat transfer and to decrease the mass in which

*Corresponding Author
E-mail Adress: dara.khalid@koyauniversity.org

Submitted: 29 January 2026; **Accepted:** 23 June 206

This paper was recommended for publication in revised form by Editor-in-Chief Ahmet Selim Dalkılıç

thermal energy is stored. Numerical analysis based on computational fluid dynamics (CFD) has confirmed the impact of fin and heat sink geometry on heat dissipation patterns [5,7]. This also involves manipulating fin spacing to enhance heat flux. Tight spacing (2.8 mm) restricts air flow, while wider spacing (14.6 mm) reduces the overall surface area. Both designs increase thermal resistance; intermediate spacing, such as 4.2 mm [4]. Another study compared the performance of circular, square, triangular, and hexagonal geometries as fins and voids. Keeping dimensions and spacing constant, circular fins proved superiority over perforated structures and other designs due to their higher surface area [8]. However, incorporating openings of any shape to the fins significantly improves heat exchange by dramatically increasing the exposed area [9,10]. Such a trend is also valid for plates, where changing their surfaces with honeycomb holes encourages heat removal [11]. Furthermore, the plate assembly pattern is crucial; parallel plates may prevent fresh air flowing in the transverse direction from reaching the core. In this regard, placing two sets of long and short rectangular fins at a right-angle prompts air invasion into the central parts of the units without the need for extra materials or space [12].

SOLIDWORKS is widely cited in research and was therefore used in the current study [13,14]. Despite many studies on optimizing heat sinks, most studies focus on specific perforation shapes and neglect key geometric parameters, such as hole depth, diameter, and the number of holes. Additionally, there is a lack of advanced regression techniques and of thorough statistical validation of model predictability. The novelty of the current paper lies in their experimental procedures and in the use of sophisticated statistical methods for analyzing the results. Drilling the core of heat sinks, instead of drilling the fins, is an innovative approach to managing thermal energy. Fitting the resulting temperature as a function of the most influential combination of diameter, depth, and number of holes using response surface method further extends earlier research. SOLIDWORKS simulations were used for temperature analysis, and the numerical results were confirmed experimentally. The findings offer reliable guidance for engineers to develop efficient cooling systems that meet the needs of energy-intensive but compact devices.

2. Theory

2.1. Numerical analysis and theoretical assumption

SolidWorks accurately analyzed the temperature distribution in the heat sinks using the finite element method under steady-state conditions. The input thermal load and the free convection coefficient of air were kept constant at 65 W and 4.8, W/m^2 respectively. The heat sinks were assumed to be isotropic, and their conductivities were temperature independent. Furthermore, any thermal resistance at the interfaces was neglected to streamline the simulation process. The governing equations for the three-dimensional temperature distribution and for convective heat flux are given by Equations 1 and 2.

$$\frac{\partial^2 T}{\partial x^2}k_{xx} + \frac{\partial^2 T}{\partial y^2}k_{yy} + \frac{\partial^2 T}{\partial z^2}k_{zz} + Q = 0 \quad (1)$$

$$q_{con} = h\Delta T \quad (2)$$

where T is temperature in °C, k is thermal conductivity in the direction of its subscript, Q is the internal heat source in W/m^3, q_{con} is the heat flux in W/m^2, and h is the convection coefficient in $W/m^2 \cdot K$.

The parameters provided in Equations 3 through 6 were used to provide a physical interpretation of the results obtained. The following are:

The Nusselt number (Nu) quantifies the efficiency of convection in the system and is given by Equation 3.

$$N_u = \frac{L_c h}{k} \quad (3)$$

Thermal R_{TH} resistance decides the system's resistance to heat transfer and is given in Equation 4.

$$R_{TH} = \frac{T_{max} - T_{min}}{q} \quad (4)$$

Grashoff (Gr) and Rayleigh (Ra) numbers were calculated using Equations (5) and (6) numbers show improved conductivity at higher values.

$$G_r = \frac{g\beta(T_s - T_\infty)L_c^3}{v^2} \quad (5)$$

$$R_a = G_r \cdot P_r \quad (6)$$

where T_{max} and T_{min} are the temperatures (°C)(of heat sinks, g is gravity, β is the thermal expansion coefficient ($1/K^0$), L_c(m) is the characteristic height, υ is the kinematic viscosity (m^2/s) and Pr is Prandtl dimensionless number.

2.2. Response surface design

The response surface method is an advanced mathematical technique used to model the relationship between independent variables and their responses. The method employs specific combinations of explanatory variables, forming a cubic shape called the design space, as shown in Figure 1. Additionally, these combinations generate specific points intended to analyze different terms of the full quadratic formula shown in Equation 7. These are the corner points (blue dots in Figure 1), which represent the maximum and minimum values of the factors; plotting them helps decide the b_i linear () and interaction b_{ij} () coefficients. The axial points (yellow) are added points defined by a design parameter known as alpha (α). These points are used to estimate the quadratic coefficients b_i. The third type, called the central point(red), is the average of the factors and handles estimating the residual (ε).

$$y = b_0 + \sum_{i=1}^{k} b_i x_i + \sum_{i=1}^{k-1}\sum_{i<j=1}^{k} b_{ij}x_i x_j + \sum_{i=1}^{k} b_{ii} x_i^2 + \varepsilon \quad (7)$$

Details of these points are provided in Table 1, with α = 1, a characteristic value of the face-centered cubic method. The value of k in the formula shows the number of factors considered in the regression, which in this case is three [15–17]. Each run was replicated three times to evaluate the pure error, and 60 runs were used for curve fitting.

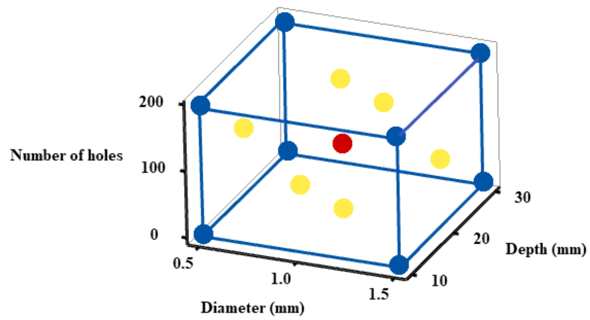

Figure 1. Design space of the response surface method

Mean relative error (MRE)was used to confirm the numerical results using the following formula:

$$MRE = \frac{1}{n}\sum_{n=1}^{n}\left|\frac{T_{experimental} - T_{SOLIDWORKS}}{T_{experimental}}\right| \times 100\% \quad (8)$$

where n is the number of observations.

Table 1. Independent factors and their levels

Parameters	Symbols	Axial	Corner	Center	Corner	Axial
Diameter (mm)	A	1	1	0.5	1.5	1.5
Depth (mm)	B	10	10	20	30	30
Number of holes	C	1	1	98	195	195

3. Experimental work

3.1. Materials selection and boundary conditions

Aluminum alloy was chosen as the heat-sink material for this paper because it offers an effective balance of high thermal conductivity (200 W/m · K), low weight, and overall cost efficiency [9]. The Ryzen 5 2400G, Thermal Design Power (TDP) of 65W, and a maximum safe operating temperature of 95°C, was selected as the CPU due to its widespread availability in the market and its predominant usage in contemporary computers. The ambient temperature and free convection coefficients were at 23°C and 4.8 $W/m^2 \cdot K$, respectively. These parameters are well set up in the open literature for free convection simulations [2,12,18,19].

3.2. Experimental setup and modeling

The shape factor of heat sinks was evaluated using circular, elliptical, and square designs. A hot plate supplied thermal power comparable to that of the conventional CPU; see Fig. 2. Voltcraft Energy Check 3000, along with a WL 202 Fundamentals of Temperature Measurement device, checked the generated energy to ensure stability. Temperatures at the interface between the hot plate and each heat sink, as well as the final steady-state temperature reached at the end of each trial, were recorded using a Type-K thermocouple connected to a Fluke 52 II Dual Input Digital Thermometer. To reduce the heat loss to the environment, glass wool insulation was placed around the hot plate. Maintaining a constant power supply analogous to real-life operating conditions is important because a crucial unit known as the integrated heat spreader (HIS) effectively stabilizes the temperature in the CPU. This allows focusing on the shape factor and perforation effects and provides validated results during the simulation phase.

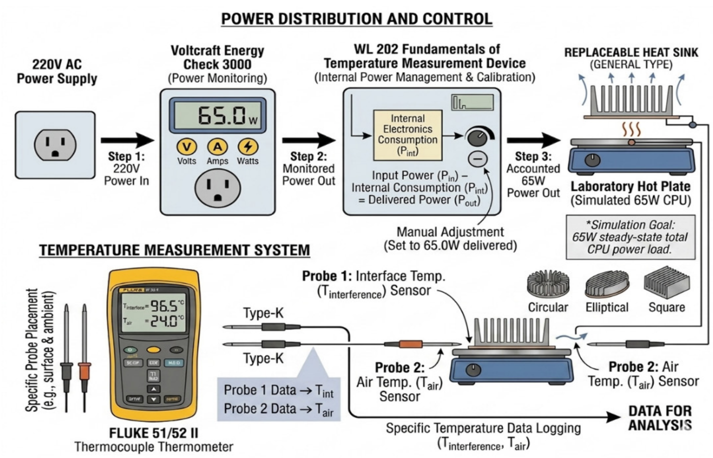

Figure 2. Setup of the experimental work

A one-kilogram concrete cube was used to set up intimate contact between the heat source and the heat sinks. To ensure free airflow, the cube featured a base with five protruding support legs. This created a space for buoyancy-driven airflow to rise through the holes and across the heat-sink surfaces. In each configuration, the stabilized lower surface temperature, mean power consumption, and time needed to reach thermal equilibrium were precisely documented.

3.3 Modification of heat sink surfaces

Perforations were introduced manually using a hand drill: 200 perforations in the circular heat sink, 195 in the square heat sink, and 95 in the elliptical heat sink, each with a diameter of 1.5 mm and a depth of 5 mm, as shown in Figure 3. A standard process for manufacturing 1.5 mm perforations was developed to keep consistency between the experimental prototype and digital models. After obtaining the real-life dimensions of each heat sink, a one-to-one-scale drilling stand was designed and analyzed using SOLIDWORKS for both perforated and non-perforated conditions under the boundary conditions previously explained.

The distance between the holes was 1 mm in all cases. The stand is then attached to the top surface of the sample to serve as a highly correct reference system. Center points were punched at each spot using a stabilized manual press before drilling to ensure positional precision and straight holes. According to post-manufacturing measurements, the discrepancy hole positions were only 0.1 mm. The uncertainty in the experimental measurements was calculated based on the accuracy of the sensing equipment. For example, during the drilling process, it was less than 2% and therefore could be neglected. On the other hand, according to the manufacturers the uncertainties of the Type-K thermocouples and the power supply were ±1.1°C (0.4%) ±5% and (not reported), respectively. By combining these factors, the overall experimental uncertainty of the temperature readings was estimated to be less than 2.5%, which is well within the acceptable range for thermal performance studies.

4. Results and discussion

4.1. Experimental results

Table 2 shows the input temperature, power, and time elapsed before the thermometer reading stabilized. Note that the key factor was that the same amount of energy was applied to all heat sinks to assess their heat-dissipation performance under constant energy input. Radiation was neglected to focus on convective efficiency. The results obtained clearly proved the role of part designs. The square shape significantly enhanced heat transfer, reducing the maximum temperature by 40.8°C and 33.6°C compared to the elliptical and circular designs, respectively. The cooling process was further enhanced by drilling 195 holes in the square structure, resulting in an added temperature drop of 5.4 °C. Similarly, the circular and elliptical shapes, with 200 and 95 holes, decreased their temperatures by 11°C and 6.2°C, respectively. Even though the results were comparable to those reported in the literature, they nonetheless showed some distinct observations. While there is general agreement about the role of shape in deciding on performance, the degree of influence varies considerably depending on specific dimensions and design details. For example, some studies favored rectangular shapes, while others preferred circular units and fins over rectangular, triangular, and hexagonal structures [6,13].

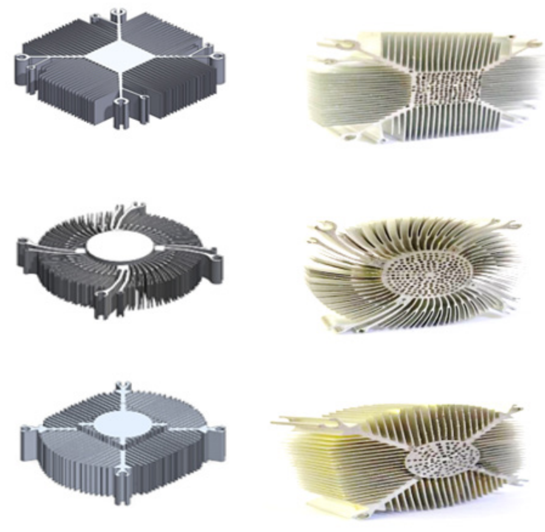

Figure 3. Heat sinks before and after perforation

Table 2. Results of the experimental works and SOLIDWORKS simulations

Type	Experimental Temperature (°C)	SolidWorks Temperature (°C)	Power (W)	Time (s)	Number of holes	
Square	137.4	132.0	66.54	53.36	-	Without drilling
Circular	171.0	176.0	66.29	55.40	-	
Elliptical	178.2	174.0	65.86	55.18	-	
Square	128.0	128.0	66.30	53.36	195	With drilling
Circular	162.0	167.0	65.20	55.40	200	
Elliptical	172.0	174.0	67.50	55.18	95	

However, the square design stays superior to the elliptical and circular designs even after drilling. The maximum temperature of the square heat sink was lower than those of the circular and elliptical heat sinks by 44°C and 34°C, respectively. This behavior is governed by the modulus (V / A), where V denotes the volume and A is the surface area. Reducing the modulus benefits heat dissipation due to the increased surface area relative to the thermal storage volume. The moduli of the square, circular, and elliptical designs were 0.575, 0.640, and 0.712 mm, respectively. This shows that engineers should adopt designs with the lowest possible modulus when manufacturing cooling units intended for compact electronic devices running under passive (fan less) cooling conditions.

Thermal resistance could further explain the behaviors seen in temperature analysis because the lower the resistance, the better the performance. The reduction in thermal resistance confirmed the impact of the design and the perforation on performance, as it decreased from 1.72 K/W to 1.58 K/W owing to the increased surface area after drilling. Furthermore, Nu supported the findings: the square design yielded the highest Nu (5.56), followed by the elliptical (5.07) and circular (4.16) designs. Greater height and an optimized perforated square core eased a robust natural convection regime compared with shorter, less efficient geometries. The lowest RTH, along with the highest Gr and Ra numbers, confirmed the superiority of the square shape.

Table 3. Comprehensive thermal and dimensionless analysis of heat sink geometries

Heat Sink Type	Height (Lc) [mm]	R_{TH} [K/W]	Nu	Grashoff (Gr)	Rayleigh (Ra)	Flow Regime
Square (Solid)	30.10	1.72	5.56	$2.51x\ 10^4$	1.78×10^4	Laminar
Circular (Solid)	22.54	2.23	4.16	1.06×10^4	7.55×10^3	Laminar
Elliptical (Solid)	27.48	2.36	5.07	1.92×10^4	1.36×10^4	Laminar
Square (Drilled)	30.10	1.58	5.56	2.51×10^4	1.78×10^4	Laminar
Circular (Drilled)	22.54	2.13	4.16	1.06×10^4	7.55×10^3	Laminar
Elliptical (Drilled)	27.48	2.21	5.07	1.92×10^4	1.36×10^4	Laminar

The SOLIDWORKS program was used to simulate heat transfer after developing new designs that perfect system performance. The overlap of the standard error bars confirmed the simulation results for which the deviation was less than 5°C , see Figure 4. Further, the MRE was 4.3%, which, given complexity of the heat sink designs, is acceptable considering that the authors manually measured the components' dimensions to build the digital models. Therefore, the authors will go ahead with upgrading the square heat sink, aided by a computer, solely because of its clear superiority.

4.2. SOLIDWORKS results

The results of the SOLIDWORKS simulation are shown in Table 4. The outputs of the replicated designs were identical, confirming the accuracy of the simulation process and cutting unexplained (pure) errors. Therefore, testing for lack of fit of the fitted models was impossible, and their probabilities (p-values) were marked with asterisks.

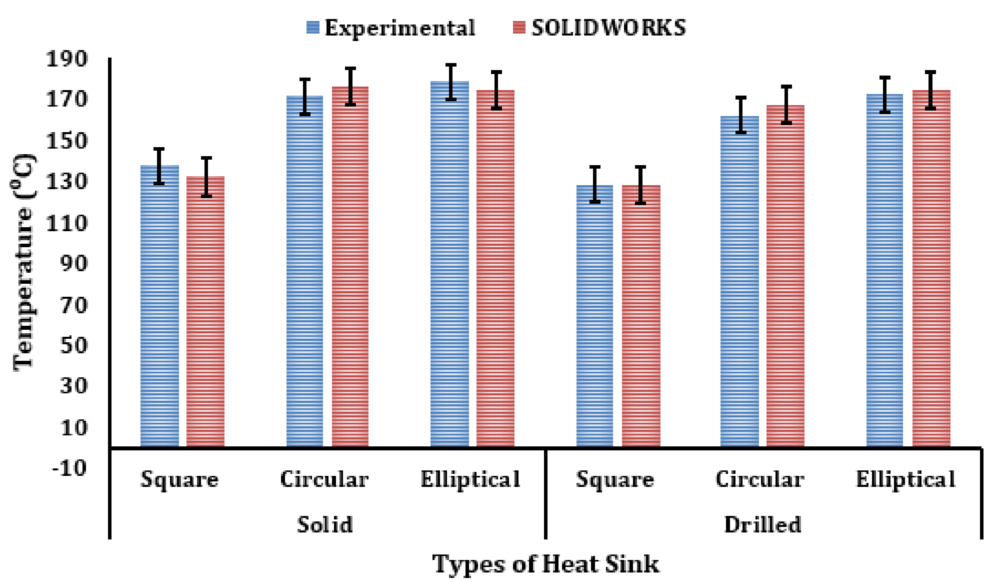

Figure 4. Results of the experiment and simulation with standard error bars

Advanced statistical filtering was used to assess and improve the predictive performance of models developed using Minitab software. For example, statistically insignificant terms were filtered out using backward elimination at a significance level of 5%. Additionally, the significance of the terms passing the filtering process was confirmed by p-values from ANOVA F-tests. Their p-values were approximately zero, showing their influential role in the models. Furthermore, the variance inflation factor (VIF) for all terms was equal to one, showing no multicollinearity among them. This is crucial for clearly interpreting the factors' effects on the responses, as higher VIF values can complicate analysis and negatively affect the models' predictive efficiency, especially when the VIF exceeds 5.

Table 4. Results of SOLIDWORKS simulations

Run order	Diameter (mm)	Depth (mm)	Number of holes	Tmax (°C)	Tmin (°C)	mass (g)	V/A (mm)
R_0	0	0	0	130	118	212.86	0.575158
R_1	1	30	98	124	111	206.61	0.523454
R_2	1	20	98	126	114	208.71	0.539684
R_3	1.5	30	195	113	98.9	184.86	0.417363
R_4	0.5	30	195	124	111	209.75	0.531309
R_5	1.5	30	1	130	118	212.72	0.574191
R_6	1	20	98	126	114	208.71	0.539684
R_7	1	20	98	126	114	208.71	0.539684
R_8	0.5	10	195	128	116	211.83	0.559854
R_9	1	20	98	126	114	208.71	0.539684
R_{10}	1	30	98	124	111	206.61	0.523454
R_{11}	1.5	10	195	124	112	203.56	0.515463
R_{12}	1	20	195	122	110	204.59	0.507453
R_{13}	0.5	30	1	130	118	212.85	0.574919
R_{14}	1	20	98	126	114	208.71	0.539684
R_{15}	1	20	98	126	114	208.71	0.539684
R_{16}	1	20	195	122	110	204.59	0.507453
R_{17}	1.5	10	1	130	118	212.82	0.574832
R_{18}	1	20	1	130	118	212.82	0.57478
R_{19}	1.5	10	1	130	118	212.82	0.574832
R_{20}	0.5	30	195	124	111	209.75	0.531309
R_{21}	0.5	10	195	128	116	211.83	0.559854
R_{22}	1	20	195	122	110	204.59	0.507453
R_{23}	0.5	30	195	124	111	209.75	0.531309
R_{24}	0.5	30	1	130	118	212.85	0.574919
R_{25}	0.5	10	195	128	116	211.83	0.559854
R_{26}	0.5	10	1	130	118	212.86	0.575078
R_{27}	1.5	20	98	124	112	203.51	0.515176
R_{28}	1.5	30	195	113	98.9	184.86	0.417363
R_{29}	0.5	20	98	128	116	211.82	0.559778
R_{30}	1	20	98	126	114	208.71	0.539684
R_{31}	1.5	20	98	124	112	203.51	0.515176
R_{32}	0.5	10	1	130	118	212.86	0.575078
R_{33}	1	20	98	126	114	208.71	0.539684
R_{34}	1	20	98	126	114	208.71	0.539684
R_{35}	1	10	98	128	116	210.79	0.557032
R_{36}	1	20	98	126	114	208.71	0.539684
R_{37}	1	20	98	126	114	208.71	0.539684
R_{38}	1	20	98	126	114	208.71	0.539684
R_{39}	0.5	20	98	128	116	211.82	0.559778
R_{40}	1	30	98	124	111	206.61	0.523454
R_{41}	1	10	98	128	116	210.79	0.557032

R_{42}	1.5	10	195	124	112	203.56	0.515463
R_{43}	1.5	30	1	130	118	212.72	0.574191
R_{44}	1	20	98	126	114	208.71	0.539684
R_{45}	1	20	1	130	118	212.82	0.57478
R_{46}	1	20	1	130	118	212.82	0.57478
R_{47}	1	20	98	126	114	208.71	0.539684
R_{48}	0.5	10	1	130	118	212.86	0.575078
R_{49}	1	20	98	126	114	208.71	0.539684
R_{50}	1	20	98	126	114	208.71	0.539684
R_{51}	1.5	10	1	130	118	212.82	0.574832
R_{52}	1.5	30	1	130	118	212.72	0.574191
R_{53}	0.5	20	98	128	116	211.82	0.559778
R_{54}	0.5	30	1	130	118	212.85	0.574919
R_{55}	1.5	10	195	124	112	203.56	0.515463
R_{56}	1.5	30	195	113	98.9	184.86	0.417363
R_{57}	1	10	98	128	116	210.79	0.557032
R_{58}	1	20	98	126	114	208.71	0.539684
R_{59}	1	20	98	126	114	208.71	0.539684
R_{60}	1.5	20	98	124	112	203.51	0.515176

Numerical simulations of the heat sinks were conducted in SOLIDWORKS 2023 using a steady-state thermal solver based on the law of conservation of energy (Figure 5). The simulations were run using the materials' data and the boundary conditions as explained previously. A curvature-based hybrid algorithm was used to generate a high-quality solid mesh and to minimize the effects of meshing on the results. For instance, the mesh of the circular heat sink consisted of 473,246 nodes and 262,943 elements.

A full factorial analysis of variance further confirmed that the proposed models adequately are the target responses. Three statistical metrics (coefficient of determination (R^2), adjusted R^2, and p-value) served as the basis for validation; see Table 5. All models] explained more than 95% of the] observed variation, as shown by their R^2 values, which supports the importance of the included terms in fitting the responses. The minimal differences between R^2 and adjusted- R^2 on one hand, and predicted- R^2 on the other, provide further evidence of the model's adequacy and cut any possibility of overfitting. Additionally, their F-test p-values were all zero, supporting the alternative hypothesis over the null hypothesis (that no model exists to describe the responses) and proving the significance of the proposed models.

Table 5. Fitted models using the response surface method

Responses	**Models**	**R^2 (%)**	**adj-R^2 (%)**	**predicted-R^2 (%)**
Tmin (°C)	114 + 4.096A + 0.2B + 0.0447C - 0.2025A.B - 0.04149A.C - 0.00233B.C	97.52%	97.24%	95.80
Tmax (°C)	126.513 + 3.489A + 0.1744B + 0.03711C -0.175A.B - 0.03866A.C - 0.001933B.C	97.86	97.62	96.29
Modulus V/A (mm)	0.54097 + 0.03398A + 0.000173B + 0.000377C - 0.00175A.B - 0.000406A.C - 0.000016B.C	97.48	97.20	95.68
Mass m (g)	200.94 + 16.75A + 0.4281 B + 0.08729 C - 4.2 A^2 - 0.4177 A.B - 0.08503 A.C - 0.002664 B.C	95.14	94.48	91.32

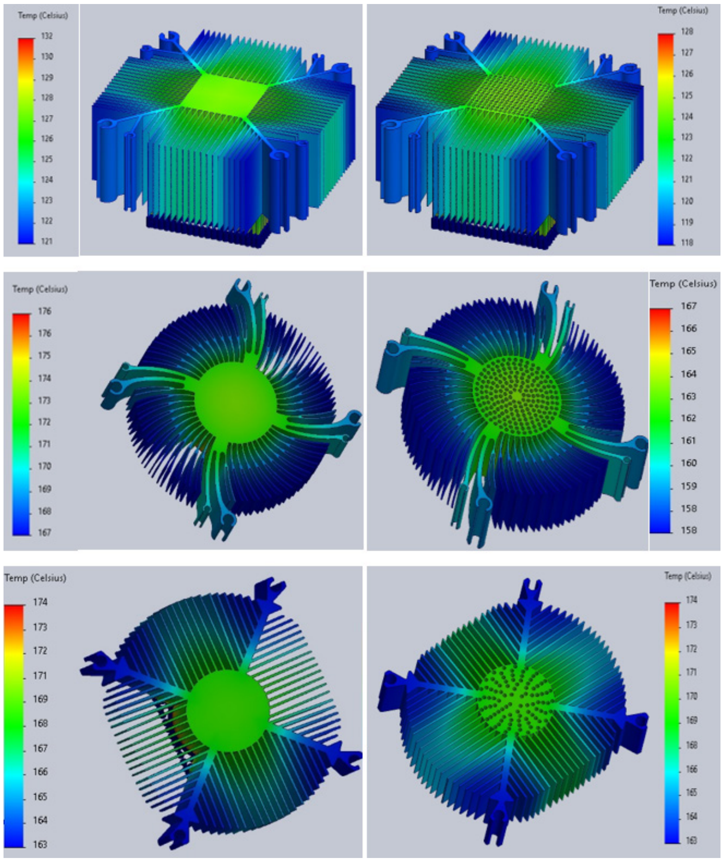

Figure 5. SOLIDWORKS results before and after drilling from top to bottom, square, circular, and elliptical heat sinks, respectively

4.3. Interpretation of the developed models using response surface methods

4.3.1. Minimum temperature of heat sinks

The output temperature (Tmin) effectively assessed the performance of the cooling systems, with a lower temperature showing better performance. An important observation is that drilling with a single hole, regardless of its size, has a negligible impact, and therefore added processing is essential to boost efficiency. The Pareto chart in Figure 6 strongly supports this conclusion, with the 'number of holes' category showing the longest bar among the variables. However, the diameter and depth of the holes also significantly influence temperature reduction.

Figure 7 proves that increasing the diameter from 0.5 to 1.5 mm and the depth from 10 to 30 mm reduces the temperature by 7.5°C when the number of holes is held constant. Additionally, drilling the heat sinks through their 30 mm thickness with 195 holes of 1.5 mm diameter reduced the temperature by 19 (unit not specified) compared with an undrilled sample. This supports the assumption that intensive drilling is essential for the best operation of low-energy electronics where built-in fans are not technically possible.

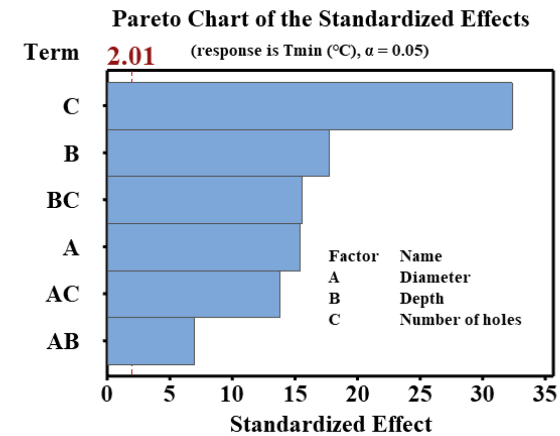

Figure 6. Pareto chart of the standardized effects of the minimum temperature

Nonlinear regression revealed that temperature depends nonlinearly on the factors considered. The signs of the coefficients reflect the direction of their effect, with positive signs showing an increasing trend. Conversely, the magnitudes of the coefficients show the intensity of those effects. The interaction between diameter, depth, and the number of holes is clear in Table 5. The factorial plots (Figure 8) are arranged in a matrix according to their coordinates (i, j), with i and j being rows and columns, respectively. The patterns of factor interactions depicted by the plotted lines strongly support their combined effects. However, it is important to note that the influence of a factor is limited by the level of another factor. For example, for up to 33 holes, neither the diameter nor the drilling depth significantly reduces the temperature, as shown in Figures 9b and 9c. The maximum temperature showed a similar trend; further discussion is unnecessary.

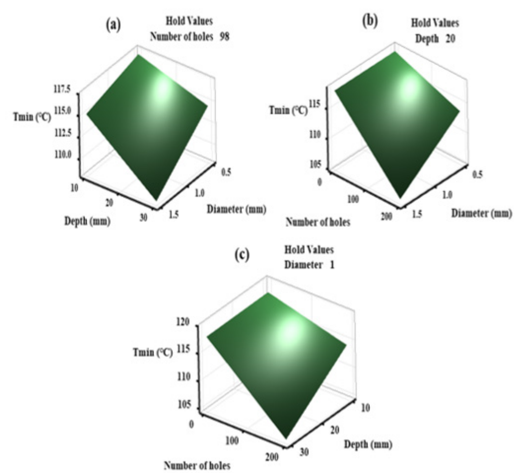

Figure 7. Response surface of minimum temperatures under the impacts of **a)** diameter and depth,**b)** diameter and number of holes, **c)** depth and number of holes

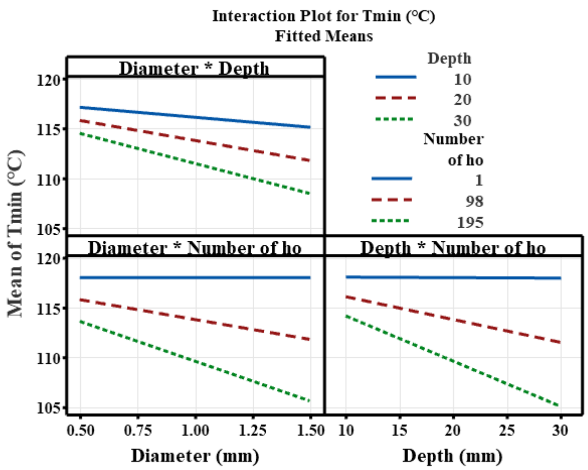

Figure 8. Factorial plot of the minimum temperature produced in the heat sink

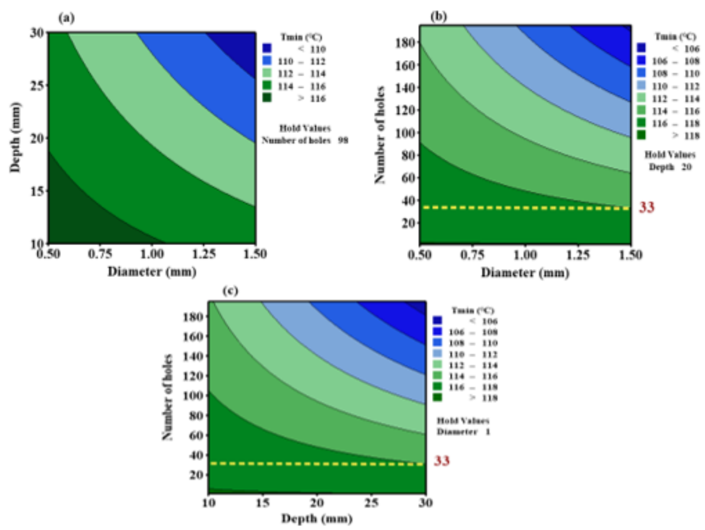

Figure 9. Contour plot of minimum temperatures under the impacts of **a)** diameter and depth, **b)** diameter and number of holes, **c)** depth and number of holes

4.3.2. Heat sinks' modulus and mass

Drilling consistently reduces the modulus, which justifies the improvement in the cooling efficiency of heat sinks [20]. For example, a structure with 195 holes of 1.5 mm diameter and 30 mm depth had a lower modulus than the control sample (R_0) by 27.4%. This was accompanied by a 13.15% reduction in mass; see R_3 in Table 3 and compare with R_0. Figures 10 and 11 highlight the role of drilling in reducing both the modulus and the mass and justify the optimization of cooling efficiency. Additionally, the Pareto charts reveal the significance of various factors, with the number of holes ranking first (see Figures 12a and 12b). Lowering the temperature by removing excess material was also cited in the existing papers and supports the current study's justifications [13].

To preserve structural durability, the perforations were limited to the solid core of the heat sink and to a depth of 5 mm, without compromising the integrity of the fins. Although the alterations led to a weight reduction of 13.15%, the integrity of the base thickness ensures that the rigidity of the heat sink is not compromised. Since the heat sink relies on natural convection and is stationary, it has no external load.

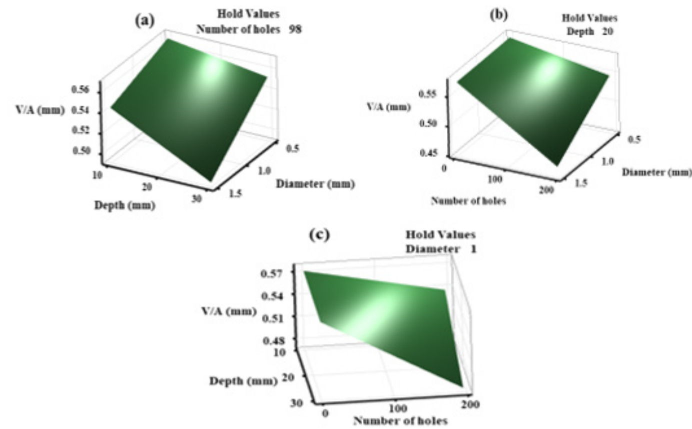

Figure 10. Response surfaces of heat sink's modulus under the impacts of **a)** diameter and depth, diameter and number of holes, **c)** depth and number of holes.

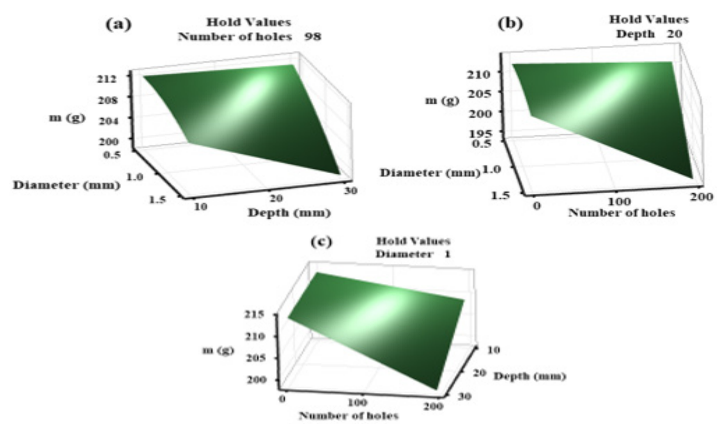

Figure 11. Response surfaces of heat sink's modulus under the impacts of **a)** diameter and depth, diameter and number of holes, **c)** depth and number of holes

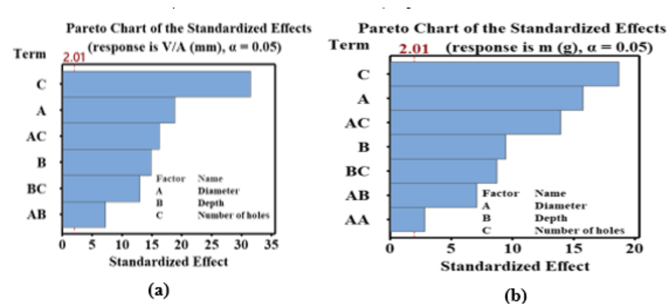

Figure 12. Pareto chart of the standardized effects of heat sink's **a)** modulus **b)** mass

4.5. Regression of temperature on modulus and mass

Regression provides insight into the temperature variations in response to the modulus and mass of heat sinks. This is essential for fully understanding the ongoing interactions between them and for providing a more detailed physical explanation of the intended purpose of drilling. In this context, the linear model adequately represented temperature variation as a function of the modulus.

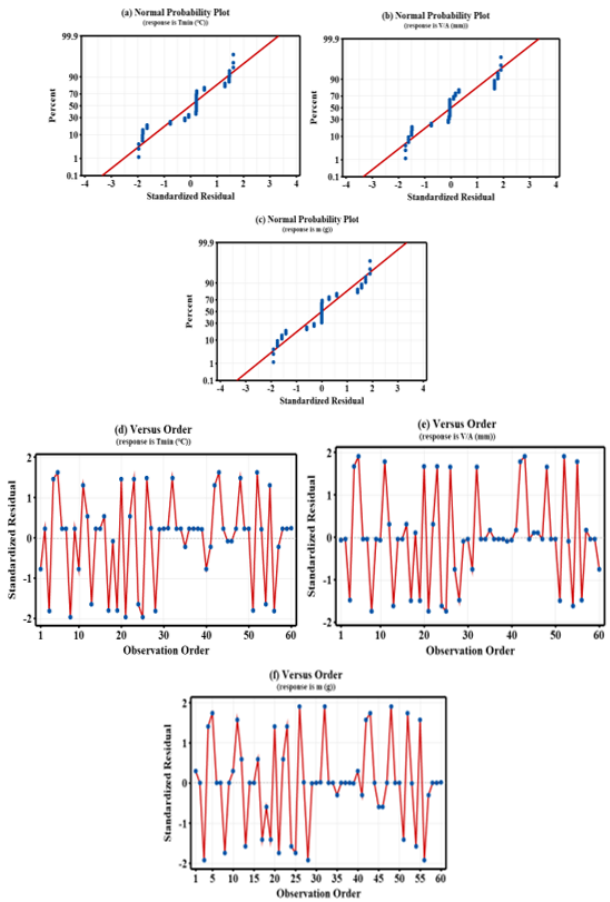

Figure 13. Fitted curves of temperature as a function of **a)** modulus **b)** mass

The proportionality shown in Figure 13a illustrates the extent to which the modulus influences temperature. On the other hand, the temperature was characterized as a cubic function of mass. The p-values from ANOVA emphasize the importance of the higher-degree terms in the model. Both models successfully achieved at least 94.91% of the observed data and this strongly supports their predictive ability (see Table 6). Figure 13 shows an attractive behavior that deserves in-depth discussion. The observed data clustered around the upper end of the curves, except for a single point. It perfected the cooling performance of the heat sink by extending the curves to the lowest temperature. This point corresponds to the most intensive drilling condition, in which 195 holes were drilled to the greatest depth and the largest diameter of 30 and 1.5 mm, respectively.

Table 6. Results of regression analysis

Model	(%)	Linear p-value	Quadratic p-value	Cubic p-value
	98.10	0.000	-	-
	94.91	0.000	0.016	0.000

4.6. Evaluating model adequacy

Normal-probability and versus-order plots were used to assess the accuracy of the mathematical expressions for prediction. In all cases, the data points are distributed around the reference(red)line, showing that the errors are normally distributed (see Figures 14a through 14c). Furthermore, the residuals fluctuate randomly around the zero line without forming any specific pattern. The observed in Figures 14d–f supports the statistical theory of error independence across the entire range of working conditions. Overall, the proposed models successfully stood for the responses [15,21]. Nevertheless, certain trends in the figures require further clarification. For example, the stacking of data in normal probability plots and flat segments at zero line in the residual plots are caused by negligible errors during replication, confirming the precision of SolidWorks in replicated simulations [22].

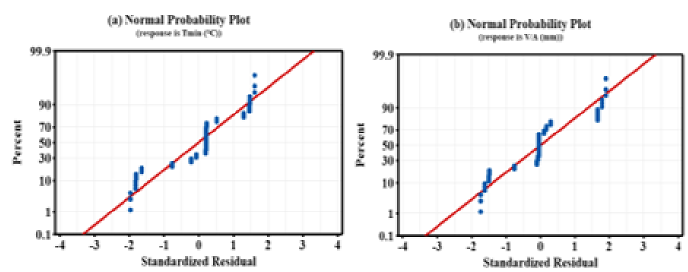

Figure 14. Normal probability plots and residual plots of minimum temperature, volume to area ratio, and mass as shown above each figure

5. Conclusions and future work

5.1. Conclusion

The design of heat sinks is crucial to improving their performance in protecting electronic devices from thermal damage. Three shapes of heat sinks are commonly available on the market: square, circular, and elliptical. This study aimed to analyze the shape factors and to suggest added simple but influential improvements to existing designs through drilling. The combined influence of the drilling parameters (diameter, depth, and number of holes) was modeled using systematic statistical regression to develop models. This attempt fills the research gap highlighted in literature and extends ongoing efforts to perfect cooling systems. After confirming the numerical results against experimental data, SOLIDWORKS 2023 was extensively used to simulate the heat-sink functions under reliable operating conditions The response surface method developed mathematical expressions for temperature as a function of the considered factors. The research concluded with findings that could serve as a scientific foundation for future developments and provide manufacturers with the knowledge needed to create eco-efficient heat sinks; these findings are summarized as follows:

1. Heat sink designs directly decide the modulus; it is a critical feature that outlines cooling performance. The square, circular, and elliptical designs are ordered from lowest to highest modulus values. Because a lower modulus eases heat transfer, the square shape is superior, reducing temperature by 40.8°C and 33.6 °C compared with elliptical and circular heat sinks, respectively.
2. Perforation enhances heat transfer by increasing the exposed surface area and reducing thermal mass. This results in an added temperature drop of 5.4°C, 9°C, and 6.2 °C after drilling the square, circular, and elliptical heat sinks with 195, 200, and 95 holes, respectively. Furthermore, the square heat sink kept its superiority after drilling, and the performance ranking among the heat sinks remained unchanged.
3. The highest Nusselt number (5.56) and the lowest thermal resistance (1.72 K/W) confirmed the superiority of the square design. The Grashoff and Rayleigh numbers further confirmed these conclusions.
4. SOLIDWORKS analysis shows that drilling the square heat sink throughout its thickness with 195 holes of 1.5 mm diameter could reduce the temperature by more than 19°C compared to the undrilled control sample.
5. The interactions among the factors (diameter, depth, and number of holes) and their quadratic terms caused the observed nonlinear behavior in the developed mathematical model. Additionally, the coefficient of determination (R^2) values exceeding 95% and p-values well below 5% statistically confirm the model's predictive capability and the significance of the included factors.
6. The resulting temperature varied linearly with the heat-sink modulus, yielding a coefficient of determination of 98.1%, compared with 94.1% for the cubic-polynomial mass model.

5.2. Future perspectives

The study examined the interactive effects of the shape parameters depth, diameter, and number of holes of square, circular, and elliptical holes on heat transfer. However, it is essential to employ advanced drilling techniques to create more complex perforations and to investigate their cooling performance. The authors suggest using electrical discharge drilling, laser drilling, and other techniques to produce slots and pentagonal or hexagonal shapes, and to compare these with classical holes. Furthermore, it is important to consider the influence of the newly developed designs on the fluid's pressure drop and their effect on the performance of heat sinks.

Acknowledgements

The authors wish to appreciate the technical staff at Koya University for their kind cooperation during the experimental phase to usefully complete the research aims.

Authorship contributions

Authors equally contributed to this work.

Data availability statement

The authors confirm that the raw data that supports the findings of this study are available within the article.

Conflict of interest

The author declared no potential conflicts of interest with respect to the research, authorship, and/or publication of this article.

Ethics

There are no ethical issues with the publication of this manuscript.

References

[1] I.T. Nazzal, T.K. Salem, S.S. Farhan, T.A. Tahseen, Investigation into the heat sink performance of the inline and cut cross fins types using different aluminum alloys, J. Therm. Eng. 10(2024)10–20. https://doi.org/10.18186/thermal.1428967.

[2] H.S. Sultan, K.B. Saleem, B.M. Alshammari, M. Turki, A. Aydi, L. Kolsi, Case Studies in Thermal Engineering Numerical investigation of natural convection from a horizontal heat sink with an array of rectangular fins, Case Stud. Therm. Eng. 61(2024)104877. https://doi.org/10.1016/j.csite.2024.104877.

[3] Huang, H., Zhai, Y.,Li, Z., Li, Y., H. Wang, Thermal management for microelectronic chips under non-uniform heat flux with supercritical CO_2. International Journal of Heat and Mass Transfer., Int. J. Heat Mass Transfe. 236 part 1(2025). https://doi.org/https://doi.org/10.1016/j.ijheatmasstransfer.2024.126271.

[4] M. Basiri, H.R. Goshayeshi, I. Chaer, H. Pourpasha, S.Z. Heris, Experimental study on heat transfer from rectangular fins in combined convection, J. Therm. Eng. 9(2023)1632–1642. https://doi.org/10.18186/thermal.1401534.

[5] R.M. and Dr.P.Govindarajan, Department, Thermal Analysis of CPU with variable Heat Sink Base Plate Thickness using Thermal Analysis of CPU with variable Heat Sink Base Plate Thickness using CFD, Int. J. Comput. Internet Manag. 18(2010)27–36.

[6] S. Ravikumar, P.S. Chandra, R. Harish, T. Sivaji, Experimental and Transient Thermal Analysis of Heat Sink Fin for CPU processor for better performance Experimental and Transient Thermal Analysis of Heat Sink Fin for CPU processor for better performance, in: IOP Conf. Ser. Mater. Sci. Eng. Pap., 2017. https://doi.org/10.1088/1757-899X/197/1/012085.
[7] F. Toapanta-ramos, M.G. Rubio, F. Ortega-loza, Numerical Study of 3D Heat Transfer in Heat Sinks with Circular Profile Fins Using CFD, Process. 13(2025)1–17. https://doi.org/https://doi.org/10.3390/ pr13103199 Copyright:
[8] T.T. Göksu, Investigation of pin and perforated heatsink cooling efficiency and temperature distribution, J. Therm. Anal. Calorim. 149(2024)6517–6529. https://doi.org/10.1007/s10973-024-13078-8.
[9] A. Kumar, A.K. Singh, P.A. Verma, Steady State Thermal Analysis of Heat Sinks having Different Types of Fins with Different Types of Perforation Using ANSYS, IJARIIE. 8(2022)5531–5544.
[10] A.S. Tijani, N.B. Jaffri, ScienceDirect ScienceDirect ScienceDirect Thermal analysis of perforated pin-fins heat sink under forced convection pin-fins condition Thermal analysis of perforated heat sink under forced convection condition Costing models for capacity optimization in I, Procedia Manuf. 24(2018)290–298. https://doi.org/10.1016/j.promfg.2018.06.025.
[11] M.I. Wani, A. Shinde, Steady State Thermal Analysis of Perforated Honeycombplate Fin, Int. J. Adv. Res. 10(2022). https://doi.org/10.21474/IJAR01/15091.
[12] S. Feng, S., Sh, M., Yan, H., Sun, F. Li, T.J. Jian., Natural convection in a cross-fin heat sink, Appl. Therm. Eng. 132(2018)30–37. https://doi.org/10.1016/j.applthermaleng.2017.12.049.
[13] S.S. Talabani, Analyzing Thermal Efficiency with Pin Fins, Perforated Bases, SolidWorks 2023 Transient Analysis, Aro-the Sci. J. Koya Univ. XIV (2025)22–30. https://doi.org/10.14500/aro.12357.
[14] N.H. Dipu, M.H. Apu, P.P. Chowdhury, Optimization of the Desktop CPU' s Straight Heatsink via CFD Simulation by SolidWorks Flow Simulation, Int. J. Pioneer. Technol. Eng. 4(2025)1–16.
[15] A.T. Azeez, M.S. Hassan, A.A. Attiyah, Modelling the complementary role of inert slag aggregate and waste glass on concrete mechanical strengths using the response surface and design-of-experiment approach, Constr. Build. Mater. 409(2023)134199. https://doi.org/10.1016/j.conbuildmat.2023.134199.
[16] A.T. Azeez, M.S. Hassan, A.A. Atiyah, Optimization of the thermal and mechanical properties of concrete with steel slag coarse aggregates and waste glass replaced with cement, Innov. Infrastruct. Solut.(2024). https://doi.org/10.1007/s41062-024-01773-2.
[17] D.K. Khidir, S.A. Atrooshi, Taguchi Method for Investigating the Performance Parameters and Exergy of a Diesel Engine Using Four Types of Diesel Fuels, Aro-the Sci. J. Koya Univ. IV (2008). https://doi.org/10.14500/aro.10101.
[18] A.A. Khalaf, H.S. Sultan, F.A. Abood, An Experimental Study of Natural Convection Heat Transfer from a Horizontal and Slightly Inclined Plate-Fin Heat Sink, Basrah J. Eng. Sci. 23(2023)98–105.
[19] E. Sinson, R. Kumar, A. Chennapragada, Heat Transfer Coefficient for a Finned CPU Heat Sink Under Natural Convection, in: Comsol Conf. 2024 Bost., 2024: pp. 1–7.
[20] M. Zunaid, A. Jindal, D. Gakhar, A. Sinha, Numerical Study of Pressure Drop and Heat Transfer In a Straight Rectangular and Semi Cylindrical Projections Microchannel Heat Sink, J. Therm. Eng. 3(2017)1453–1465.
[21] I. Kattoof, M.S. Hassan, S.S. Hasan, Effects of Liquid Nitrogen Cooling on the Microstructure Properties of Nano - Modified Concrete Under Hot Conditions, Arab. J. Sci. Eng. (2022). https://doi.org/10.1007/s13369-021-06496-5.
[22] R.H. Myers., D.C. Montgomery., C.M. Anderson-Cook., Response Surface Method, 3rd Editio, John Wiley & Sons, 2009.